Abstraction of Oxygen from Dioxygen on Al(111) Revealed by Resonant Multiphoton Ionization Laser Spectrometry†

Marcello Binetti‡ and Eckart Hasselbrink*

Fachbereich Chemie, Universität Essen, D-45141 Essen, Germany

Received: February 22, 2004; In Final Form: May 11, 2004

Molecular beams and laser spectroscopy have been used to prove the operation of an abstraction channel in the interaction of oxygen molecules with the Al(111) surface. In this process, one O atom is adsorbed on the surface whereas the other remains in the gas phase. Experiments find that abstractive chemisorption is operative at all translational energies and markedly increases with energy while rotational excitation of the molecules suppresses the abstraction process. The gas-phase oxygen atoms have a translational energy about 1/7 of the excess energy from the reaction.

Introduction

The chemical interaction of oxygen with metal surfaces attracts considerable interest since it underpins many technical applications in areas such as catalysis, microelectronics, and environmental sensing. In semiconductor device fabrication the peculiar properties of thin aluminum oxide films are utilized, e.g., to make gate oxides, for electrical insulation and for migration prevention. Nevertheless, the microscopic steps of O_2 dissociative adsorption, surface migration, and bulk penetration, eventually leading to oxide formation, are only rudimentarily understood.[1] The initial steps of oxide formation have recently been studied experimentally[2] and theoretically[3] by several authors. The very first step, dissociative adsorption, has been an experimental puzzle. It is generally accepted that the initial sticking coefficient at thermal energies is small ($s_0 < 10^{-2}$) and increases with translational energy to reach 0.9 at 0.9 eV.[4] Moreover, Österlund et al. report that vibrational excitation of the molecules enhances the sticking, whereas it is unaffected by the sample temperature. On the contrary, Zhukov et al.[2] have proposed the existence of a molecular precursor to rationalize an observed temperature dependence in their X-ray photoelectron spectroscopy (XPS) study on oxide formation. In a recent molecular beam experiment no direct evidence for such a precursor state has been found, setting an upper limit of 0.1 eV to its binding energy.[5] Also, Hofmann et al.[6] did not observe a molecular chemisorption state when heating an O_2-covered sample from 40 K.

Experimentally, it has been established that abstractive chemisorption is an important reaction channel in the early steps of aluminum oxidation. Combining results from scanning tunneling microscopy (STM) studies and laser spectroscopic analysis of the scattered flux, it has been shown that the abstraction channel is dominating at low translational energies.[7] In this process, only one of the O atoms is adsorbed while the other remains in the gas phase. Abstractive and ordinary chemisorption can be discriminated by STM since either single adsorbed oxygen atoms or pairs of such atoms result. In their seminal work Brune et al.[8] found that single oxygen atoms are observed by STM when an Al(111) surface is exposed to thermal O_2 at room temperature. This finding, questioned by Schmidt et al.,[9] has recently been confirmed by Komrowski et al.[7] and Dalidchik et al.[10]

At higher energies ordinary dissociative chemisorption also proceeds; in this case both of the atoms are adsorbed with only a small distance separating them. The total sticking probability at thermal energies is small ($s_0 \approx 10^{-2}$) and rises sharply with increasing translational energy to reach 0.5 at 0.2 eV and to saturate with 0.9 at 0.9 eV.[4] The ratio of abstraction to ordinary chemisorption events observed by STM changes smoothly from 15 at a translational energy of 25 meV to 2 at $E_{trans} = 0.8$ eV.[7]

These results are in stark contrast to the predictions made by up-to-date density functional theory (DFT). Unanimously, these calculations predict nonactivated adsorption[11,12] that should result in a sticking coefficient close to unity even at low translational energies. According to these calculations, abstraction could only be a minority event. Hence, it has become evident that the interaction of O_2 with Al(111) cannot be described by those methods which have successfully been applied to O_2−transition-metal systems.[13] This conflict has been interpreted to point to the significance of nonadiabatic effects in the adsorption of oxygen on Al(111), which are beyond the scope of the present DFT codes.[14] It is suggested that at low translational energies the O_2 molecules stay on the diabatic potential energy surface. It has been proposed that the abstraction channel results when molecules approach the surface in the upright geometry, which is favorable for charge transfer. Rapid transfer of two electrons leads then to bond fission where one of the atoms may be expelled into the gas phase again.

In this context, a contribution from possible cannonball trajectories has also been discussed,[15,16] in which case the second oxygen atom is initially ejected from the adsorption site but later recaptured by the surface. Indisputable experimental evidence for this channel has not yet been demonstrated. However, it cannot be ruled out that a fraction of the abstraction events lead to cannonball trajectories. These events cannot be discriminated by STM from abstraction events if a distance exceeding approximately 50 Å finally separates the two oxygen atoms.

In this paper we present the results from a study using laser spectrometry, namely, resonant multiphoton ionization (REMPI) detection of O atoms, to unambiguously establish the operation of an abstraction channel in the interaction of molecular oxygen

† Part of the special issue "Gerhard Ertl Festschrift".

* To whom correspondence may be addressed. E-mail: eckart.hasselbrink@uni-essen.de.

‡ Present address: Fritz-Haber-Institut der Max-Planck-Gesellschaft, Faradayweg 4-6, D-14195 Berlin, Germany.

10.1021/jp049197y CCC: $27.50
Published on Web 07/02/2004

with an Al(111) surface. This paper is organized as follows: In the next section the experimental setup and procedures are described. In the following section the results are presented. In the last section we discuss the results in light of recent experimental and theoretical work. Preliminary results from this study have been published elsewhere.[7,17,18]

Experimental Section

The molecular beam scattering experiments have been performed using an ultra-high-vacuum (UHV) apparatus, previously described in detail.[19] A three-stage differentially pumped molecular beam line is used to derive from a pulsed nozzle (General Valve, Series-9) gas pulses of ~160 μs length and a peak flux of 10^{15} molecules cm^{-2} s^{-1}. For this purpose, the pulses are chopped using a home-built Fizeau-type chopper rotating at about 200 Hz and a fast aperture shutter (Uniblitz, LS6) picks individual pulses from the pulse train produced by the chopper. To be able to vary the translational energy of the beam, a ceramic tube of 4 cm length and 1 mm inner diameter has been attached by a Teflon adapter to the pulsed valve orifice. The ceramic tube can be heated to a temperature of 500 K without hampering the functionality of the pulsed valve. By furthermore seeding the oxygen molecules in He, the translational energy could be increased up to 435 meV. The translational energy of the beam has been measured by placing a mass spectrometer at two different distances along the beam. From the delay in arrival time of the gas pulse the velocity could be inferred. Using the same instrument, the beam flux has been controlled in situ before the sample is exposed to the beam. The surface was exposed to a limited number of gas pulses, to not exceed the low-coverage limit ($\Theta < 0.05$ monolayer (ML)). The scattering experiments were performed with the sample held at room temperature.

The molecular beam (diameter 6 mm) strikes the Al(111) sample at an angle of incidence of 45°. Two different Al(111) samples were used during this study. The first was the same one Brune et al. used for their experiments. The second was obtained from Monocrystals Co. and was similar to the ones used by Kummel and co-workers. The Al(111) samples (±0.5°, purity 99.999%) were cleaned by prolonged Ar^+ ion sputtering at 500 eV. The surface cleanliness was checked by Auger electron spectroscopy (AES). Sputtering cycles were repeated until the LMM Al peak (68 eV) was maximal in size. The sample was annealed to 700 K, and the order of the surface was subsequently checked by low-energy electron diffraction (LEED).

In the scattered flux of O_2 molecules, O atoms are detected by (2 + 1)-photon REMPI at 226 nm utilizing the resonant transition from the (2p) $^3P_2$ ground state through the (3p) $^3P_{0,1,2}$ state as the intermediate (Figure 1).[20] For this purpose a Nd:YAG-laser (Spectra Physics, GCR-190) pumped tunable dye laser (Sirah, Precision-Scan-G) is used to produce 452 nm light which is frequency-doubled in a β-BBO crystal, producing pulses of 2.5 mJ energy (10 ns pulse length, 0.14 cm^{-1} bandwidth). The light is focused by a 220 mm lens into the UHV apparatus, with the focus typically located 10 mm away from the sample in the direction of the surface normal (Figure 2). The laser beam runs perpendicular to the scattering plane. The focus is expected to have a diameter of 26 μm and a Rayleigh length of 10 mm. However, the experiment is relatively insensitive to the angular distribution of the O atoms released from the surface reaction due to the large diameter of the molecular beam and the short distance of the detection volume from the sample.

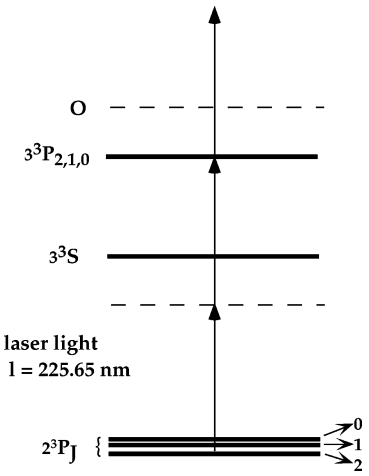

Figure 1. REMPI scheme for O detection. The transition is a (2 + 1) process with the (3p) ^3P_J state as the resonant state.

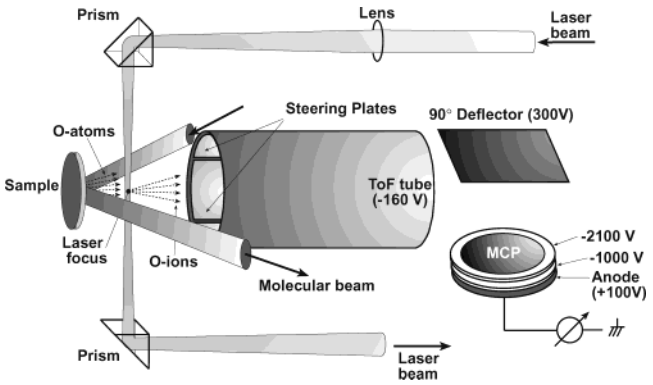

Figure 2. Experimental arrangement of the sample, molecular beam, and REMPI-TOF detector. The whole REMPI detector is mounted such that it can be moved horizontally in the drawing plane, whereby the distance between the detection volume and sample is changed.

The ions produced in the detection volume are collected by an extraction field, mass separated in a field-free time-of-flight tube, and finally detected by a chevron of channel plates (Galileo 1397-1900). Due to the low signal level, the use of conventional boxcar averagers was impractical. Instead, individual ions event are gated with an appropriately delayed window after the laser pulse and finally counted.

A small high-vacuum apparatus with a base pressure of 10^{-5} mbar is used for spectroscopic calibration experiments. The chamber is equipped with a detector identical to the one in the UHV chamber. Only the steering plates and the 90° deflector have been spared since there is no need for them. O_2 or alternatively NO_2 is bled into the chamber such that a partial pressure of 10^{-3} mbar results. This chamber is also used to tune the dye laser initially to the proper wavelength for O atom detection.

The design of this heatable pulsed nozzle has peculiar implications on the properties of the beam. First, the expansion is not as good as it would be without the attached ceramic tube, resulting in a beam flux reduced by about 1 order of magnitude. Second, the rotational cooling is not as effective as in a conventional expansion. Hence, when heating the nozzle, we expect not only the translational energy of the molecules in the beam to increase but also their rotational temperature. Direct determination of the rotational state distribution of the O_2 molecular beam is not feasible. Therefore, we resorted to measuring the rotational temperature for a beam of NO produced under the same experimental conditions using (1 + 1) REMPI

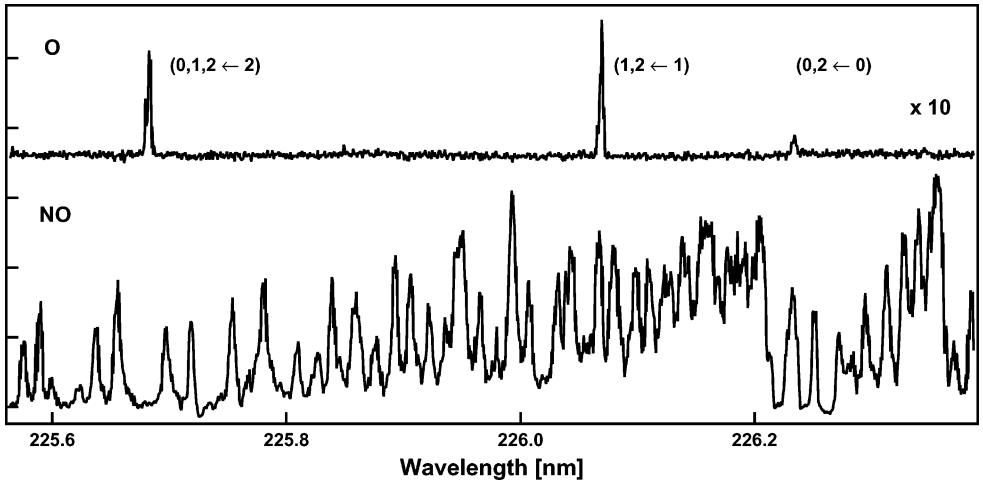

Figure 3. REMPI spectra recorded for O atom and NO molecule photofragments from 226 nm photolysis of NO_2. NO_2 photodissociation is partially influenced by 2-photon resonant excitation. The creation of the ions follows in a subsequent (2 + 1) or (1 + 1) process for O atoms and NO molecules, respectively. O atoms and NO molecules are separated by their different flight times through a time-of-flight mass filter in the REMPI detector. The O atom signal is expanded by a factor of 10.

TABLE 1: Translational and Rotational Energies of the O_2 Molecular Beam Obtained by Heating the Nozzle and Seeding in He[a]

T_{nozzle} (K)	seeding (% in He)	$\langle E_{trans} \rangle$ (meV)	T_{rot} (K)
300	100	90	36 ± 4
300	10	235	54 ± 6
500	100	135	75 ± 6
500	10	434	154 ± 7

[a] T_{Rot} is inferred from measuerements on a NO beam.

detection. Indeed, a marked increase of the rotational temperature from 36 to 154 K is observed when the nozzle is heated and the beam seeded (Table 1).

Results

The efficiency of the detection scheme has been studied using photodissociation of NO_2 as the source for O atoms. For this purpose the dye laser serves as the photolysis light source and as the probe laser. The resulting NO and O fragments can be detected in the same wavelength region. The spectrum shown in Figure 3 has been obtained using the test chamber and a focusing lens of slightly longer focal length (250 mm). The ion signal on the O atom transition has about 1/10 the strength of the molecular NO signals. Since (i) O and NO photofragments are produced in equal abundance, (ii) the latter are however distributed over about 10^2 quantum states, and (iii) the NO signal shows some saturation, it can be inferred that the O atom detection efficiency is about 10^{-2} to 10^{-3} times that of NO. We attribute this effect to the fact that O atom detection is a (2 + 1)-photon REMPI process, whereas NO detection involves only 1-photon transitions. Here, it should be noted that the bandwidth of the dye laser is comparable to the natural line width of the O atom line (0.16 cm^{-1}). Moreover, reducing the bandwidth would not necessarily have resulted in larger signals, since the bandwidth is quite adapt for the Doppler width of the expected O atom signal (0.3 cm^{-1}).

Figure 4 shows the time-of-arrival spectrum recorded by the ion detector when a beam of O_2 is directed toward the clean Al(111) surface and the laser tuned to the O atom $2^3P_{0,1,2} \leftarrow 2^3P_2$ transition at 225.655 nm. This signal has been accumulated during the first 500 gas pulses. These data have been recorded at a somewhat shorter distance (6 mm) to the crystal than typical.

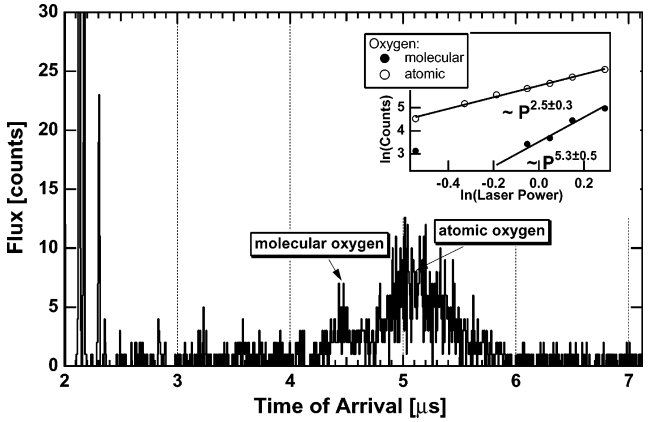

Figure 4. Time-of-arrival spectrum at the ion detector for the laser set to 225.655 nm and a laser pulse energy of 0.6 mJ/pulse. The zero point in time corresponds to the firing of the laser pulse. Two signal peaks are identified in the spectrum centered at 2.5 and 3.1 μs, respectively. The inset shows the dependence of each signal on the laser power in a log−log plot. The first peak exhibits a dependence scaling with $P^{2.5\pm0.3}$, in agreement with a 3-photon process, the latter with $P^{5.3\pm0.5}$ suggesting a 5-photon process.

For this arrangement the O_2 background pressure in the detection volume is larger. The time-resolved trace shows two features centered at 4.5 and 5.1 μs times-of-arrival, respectively. By detuning the laser wavelength, it was verified that the creation of both signals involves REMPI of oxygen atoms. Experiments at different exposure times and different placements of the laser focus with respect to the crystal lead to different weights of the two signals. To clarify their respective origin, time-of-arrival spectra have been recorded for different laser powers, P. The area attributed to each feature has been integrated. The results are displayed in the inset of Figure 4 in a double-logarithmic graph. The first peak in the time-of-arrival spectrum scales with P^n with $n = 5.3 \pm 0.5$, whereas the second scales with P^n with $n = 2.5 \pm 0.3$. This finding is consistent with the interpretation of the first peak as due to photodissociation of O_2 in the focus of the laser beam and subsequent ionization of one O atom, and the second as caused by the detection of atomic oxygen. Photodissociation of O_2 by a nonresonant 2-photon process and subsequent ionization of one O atom by a (2 + 1)-photon REMPI is a 5-photon process. This 5-photon dependence is well reflected by the data. The ionization of O atoms, which have

been formed in the abstraction process at the surface, is a (2 + 1)-photon process, which corresponds well with the power dependence of the latter signal. The experimentally determined exponent is somewhat smaller than 3, which is a frequent observation in REMPI, and due to partial saturation of the ionization step.

At 226 nm oxygen photodissociation proceeds mainly through a 2-photon excitation to the $^3\Pi_{0,1}$ state and subsequent predissociation, leading to $O(^3P_2)-O(^1D_2)$ pairs.[21] This process has an excess energy of 1.95 eV that appears as the translational energy of the released atoms. The polarization of the laser light in our experimental setup was aligned under an odd angle due to experimental constraints. The corresponding momentum of the atoms was therefore directed neither perpendicular to nor in the direction toward the time-of-flight tube. Nevertheless, half of the nascent atoms obtained a velocity component toward the time-of-flight tube. Consequently, they arrived at earlier times than atoms which were at rest prior to the ionization. The other half of the atoms had a velocity component away from the time-of-flight tube. The corresponding peaks would have been expected at about 6 μs. They were not observed, most likely since they escaped the extraction field. However, both peaks were clearly observed in a separate experiment, in which O_2 in the molecular beam was photodissociated and the sample was placed as a reflecting electrode outside of the beam.

The width of the larger peak at 5.1 μs which we attribute to detected atoms arises from (i) the velocity and angular distribution of atoms prior to ionization and (ii) the spread of flight times through the detector depending on these initial conditions.

In further experiments, only the signal of the peak attributed to the detection of atoms formed by abstraction has been integrated. All experiments have been performed with the laser on the $3^3P_J \leftarrow 2^3P_2$ line, since the signal on the other lines was much smaller. The original data have been corrected for the varying flux of the O_2 beam due to dilution in the seeding gas. For this purpose the beam flux and velocity have been determined using the mass spectrometer at the beginning of each experiment. The abstraction probability R is defined as

$$R = j_O/j_{O_2} \tag{1}$$

where j_O and j_{O_2} are the fluxes of the resulting O atoms and the incoming O_2 beam, respectively. Since the mass spectrometer is a density-sensitive detector

$$j_{O_2} \propto I_{QMS} v_{O_2} \tag{2}$$

REMPI is also a density-sensitive detection process. Hence

$$j_O \propto F(\theta) I_O v_O \tag{3}$$

where $F(\theta)$ is a factor reflecting the angular detection efficiency of the setup. We assume that the final velocity of the O atoms resulting from the abstraction process does not significantly vary with the translational energy of the incoming molecule. This assumption is supported by the consideration that the translational energies are small compared to the chemical energies involved. It is further supported by experiment as discussed below. Moreover, we assume also that the angular distribution of the released O atoms does not change that much that we could detect it with our setup, which is a safe assumption, since the setup is rather insensitive to the angular distribution. Under these assumptions the corrected REMPI signals are directly proportional to the partial sticking coefficient for the abstraction process, i.e., the probability for an incoming molecule to undergo that particular process:

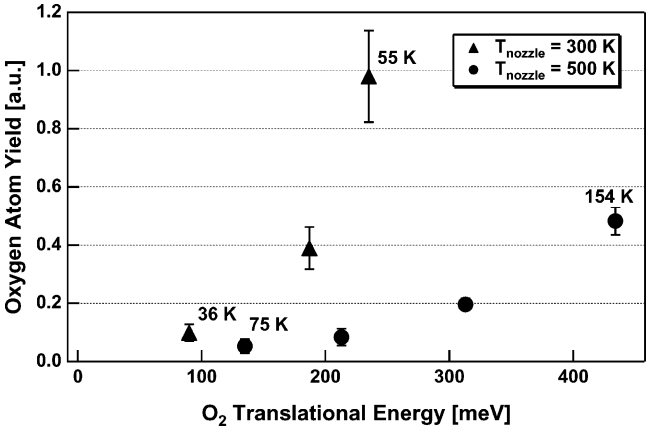

Figure 5. Partial sticking coefficient for the abstraction reaction, i.e., probability of undergoing the abstraction process per incoming molecule as a function of translational energy. The data are in relative units, since REMPI does not allow for an accurate absolute calibration. The labels at the data points indicate the rotational temperature of a NO beam at the same conditions under which the data point was recorded.

$$R(E_{trans}) \propto I_o/I_{QMS} v_{O_2} \tag{4}$$

Figure 5 shows the data obtained for the oxygen atom flux when the sample is exposed to an O_2 beam of various translational energies. Two data sets utilizing different temperatures of the molecular beam source nozzle have been obtained. Where available, we have labeled the data points with the approximate rotational temperature of the beam under the conditions at which it was recorded. The data show a strong increase of the abstraction probability with translational energy. However, the data set obtained with the nozzle heated to 500 K shows an abstraction probability consistently lower than that obtained with the nozzle at room temperature.

Figure 6 shows the temporal evolution of the signal with progressing exposure of the Al(111) sample to an O_2 beam with 0.19 eV translational energy. Each data point represents the accumulated counts from 100 laser shots. At time $t = 0$ s the beam shutter is opened. A rapid rise of the signal is observed. The rise time is real since the detection system does not induce any temporal averaging beyond that connected with the accumulation for one data point. Hence, we conclude that the yield of oxygen atoms first increases with exposure. After reaching a maximum, a rapid falloff to half the peak value is observed. Subsequently, a slow decrease of the signal with time follows. At $t = 660$ s the beam shutter is closed again. The signal settles to its zero level. We expect at $t = 660$ s an O atom coverage of about 0.2 ML. Similar data have been obtained for different E_{trans} values. The oscillatory fine structure of the signal is not reproducible, but rather an experimental artifact.

The translational energy of the O atoms released by the abstraction reaction can be inferred from the time-of-arrival spectrum observed by the REMPI detector (Figure 7). For these experiments, the distance between the sample and detection volume was set to 10 mm. Time-of-arrival spectra for different E_{trans} values showed identical onsets of the signal at approximately 5 μs and similar widths of the peak of about 0.9 μs. The equations of motion of the O ions through the REMPI detector were constructed, and the time of arrival as a function of the initial translational energy of the ion was obtained. This function was used to invert the time-of-arrival spectrum to the energy distribution function of the O ions. This energy is

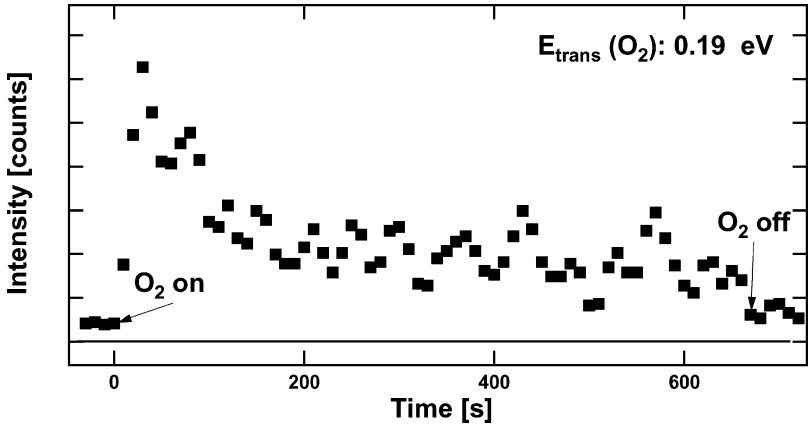

Figure 6. Temporal evolution of the O atom signal at $E_{trans} = 0.19$ eV. At $t = 0$ s the beam shutter is opened, and at $t = 660$ s it is closed again. An accumulated O coverage of 0.2 ML is expected at that point.

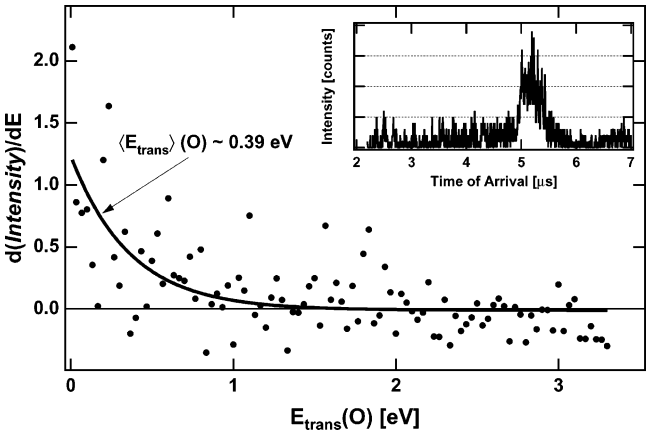

Figure 7. Translational energy distribution of O atoms released from the surface in the abstraction reaction. The inset shows the time-of-arrival spectrum of the O atoms at $E_{trans} = 0.19$ eV. The translational energy distributions is obtained by inverting the time-of-arrival spectrum according to a modeled flight path through the detector. The solid line shows a fit to the data by an exponential, yielding a mean translational energy of 0.39 ± 0.08 eV.

identical to that of the O atom originating from the abstraction process, since it is not significantly changed by the ionization process. This procedure does not take into account the different possible directions of motion of the O atoms as they pass through the detection volume. Given the distance between the sample and the ionization volume and the diameter of the sample, a spread of 27° is possible. For the spread in flight times though the detector only the passage from the ionization volume to the front of the drift tube is significant. For this time the projection of the nascent velocity onto the center line of the detector is relevant. Hence, our procedure somewhat underestimates the O atom translational energies. A thorough analysis yields that this error is about 15%. The resulting translational energy distribution was fit by an exponential function from which the average translational energy, $\langle E_{trans}\rangle$(O), was obtained. Experiments for different translational energies of the impinging O_2 beam yield $\langle E_{trans}\rangle(O) = 0.4 \pm 0.1$ eV without any indication of a dependence on the translational energy of the incoming molecule (Table 2).

Since the detection efficiency is largely insensitive to the angular distribution for the O atoms released in the surface scattering event, it was possible to study the dependence on the angle of incidence of the O_2 molecular beam. For this purpose the sample was rotated and moved along the molecular beam, while the time-of-flight (TOF) detector was repositioned

TABLE 2: Translational Energies for O Atoms, $\langle E_{trans}\rangle$(O), Emitted during the Initial Oxidation of Al(111) for the Incident Translational Energy $\langle E_{trans}\rangle$ of the O_2 Beam

$\langle E_{trans}\rangle(O_2)$ (meV)	$\langle E_{trans}\rangle$(O) (meV)	$\langle v\rangle$(O) (m/s)	$\langle E_{trans}\rangle(O_2)$ (meV)	$\langle E_{trans}\rangle$(O) (meV)	$\langle v\rangle$(O) (m/s)
90	360 ± 83	2083	190	392 ± 83	2173
135	376 ± 88	2128	310	385 ± 78	2154

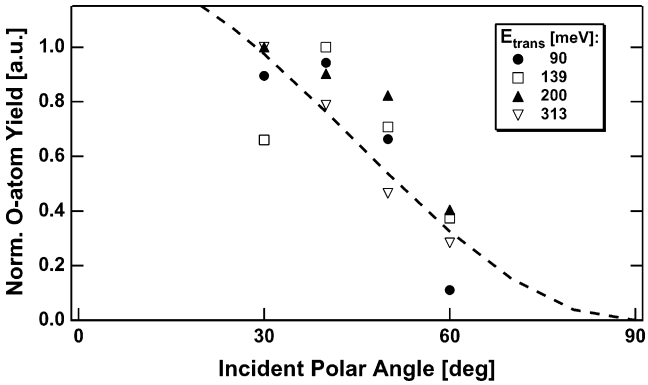

Figure 8. O atom yield vs O_2 incident polar angle. The data for the different O_2 translational energies have been normalized. Due to experimental constraints it was not feasible to record the data for angles smaller than 30°. The dashed line represents a $\cos^2\theta$ curve.

to leave unchanged the relative distance between the laser focus and metal surface. The range of angles over which the experiment was possible was limited by the observation that the extraction field for the O ions became too distorted when angles smaller than 30° were probed. Figure 8 shows the data obtained for angles between 30° and 60°. The data for the different translational energies have been normalized. In the limited range experimentally accessible, the data are consistent with a $\cos^2$ dependence on the angle of incidence as would result from normal energy scaling.

Discussion

The laser spectrometric data presented in this paper constitute direct evidence for the ejection of O atoms during exposure of an Al(111) surface to O_2 molecules. The data presented in Figure 4 show that it is possible to discriminate between O atoms produced by photodissociation of O_2 from the background gas and O atoms released by the surface reaction. The presented work constitutes the first direct evidence of an abstraction pathway in the dissociative chemisorption of O_2 on Al(111), thereby proving a hypothesis originally proposed by Wahnström et al.[16] to rationalize the STM findings of Brune et al.[8]

The REMPI results are also complementary to the STM data of Kummel and co-workers,[7,17] who studied the chemisorption of oxygen on Al(111) at room temperature, exposing clean metal surfaces to O_2 from a molecular beam with energies ranging from thermal to 0.8 eV. They observed predominantly single adsorbed oxygen atoms when the sample was exposed to thermal energy O_2. At high translational energies singles and pairs were observed with nearly equal probability. In view of the data presented in this paper the singles are interpreted as the counterpart to the O atoms detected by REMPI.

It is not feasible to determine the absolute probability of the abstraction process by REMPI. Hence, its yield can only be inferred from the STM experiments. The data reported here are consistent with an absolute sticking coefficient of approximately 10^{-2} at thermal energies as reported by Österlund et al.[4] and a large predominance of the abstraction process under these conditions as observed by STM.

The data presented in this paper show a marked increase of the abstraction sticking coefficient with translational energy. However, heating of the nozzle is counterproductive. This is so far surprising, as it indicates that increasing the energy of the molecules reduces the probability for the abstraction process. It can be ruled out that the change in population of molecular vibrational levels is the cause for this effect. If we assume for the moment that no vibrational relaxation in the beam expansion occurs, then the population in $v = 1$ increases from 7×10^{-4} to 1×10^{-2} when the gas temperature is increased from 300 to 500 K. In fact, we expect some vibrational cooling to occur such that the population of this state will be even smaller. The population in even higher vibrational states is negligible ($<10^{-4}$). Thus, regardless of the nozzle temperature, 99% of the molecules are in the vibrational ground state. We conclude that it is impossible to explain the reduction in abstraction probability by a depletion of the vibrational ground state. Hence, the observed effect has to be explained on the basis of the rotational state distribution in the beam.

It is problematic to infer the rotational state distribution of the O_2 beam from measurements on a NO beam, since the first is a homonuclear and the latter a heteronuclear molecule. Therefore, the first can only undergo $\Delta J = \pm 2$ transitions for which the cross sections are smaller than for $\Delta J = \pm 1$ transitions, which limits the rotational cooling rate. The rotational cooling of O_2 in a beam has been measured by Reuss and co-workers.[22] Andresen and co-workers have studied pulsed NO beams and the rotational energy transfer of that molecule.[23] They found that also NO prefers $\Delta J = \pm 2$ transitions; i.e., it behaves closely similarly to a homonuclear molecule. Hence, it is reasonable to expect that the NO beam will have properties similar to those of the O_2 beam, since the mass and moment of inertia of NO and O_2 differ by only 6.5%.

Apparently, a reduction by a factor of 3 in the probability for the abstraction reactions results when the rotational temperature increases from 50 to 150 K. A similar albeit much subtler effect has also been observed in the dissociative adsorption of H_2/Cu and H_2/Pd(111).[24] For the further discussion we define the property

$$F(J_{\max},T_{\mathrm{rot}}) = \frac{\sum_{J=0}^{J_{\max}}(2J+1)\exp[-E_{\mathrm{rot}}(J)/kT_{\mathrm{rot}}]}{\sum_{J=0}^{\infty}(2J+1)\exp[-E_{\mathrm{rot}}(J)/kT_{\mathrm{rot}}]}$$

where $E_{\mathrm{rot}}(J) = B_{\mathrm{rot}}J(J+1)$ is the rotational energy of state J and T_{rot} the rotational temperature. This property quantifies the fraction of the population in rotational states $J = 0$ to $J_{\max}$ at a given temperature. Using the parameters for molecular oxygen in the ground state ($B_{\mathrm{rot}} = 1.4456\ \mathrm{cm}^{-1}$), we obtain $F(J_{\max}=1,T_{\mathrm{rot}}=35\mathrm{K}) = 0.25$ and $F(J_{\max}=1,T_{\mathrm{rot}}=155\mathrm{K}) = 0.062$; i.e., the fraction of molecules in the lowest two rotational states is reduced by a factor of 4. This ratio is in good qualitative agreement with the observed reduction in abstraction probability. A quantitative comparison is hampered by the fact that there are no data available for two rotational temperatures at the same translational energy. However, interpolating the data at $E_{\mathrm{trans}} = 0.2$ eV, we estimate a ratio of 6:1 for the abstraction probability at rotational temperatures of appoximately 47 and 90 K. Hence, we conclude that the experimentally observed effect is even somewhat larger, suggesting that abstraction is effectively impaired for molecules in rotational states with $J \geq 2$.

The final translational energy of the O atoms is found to be 0.4 ± 0.1 eV. This value is a small fraction of the available excess energy of 2.8 eV.[25] The low translational energy might result from the concerted motion of the incoming molecule and the substrate atoms upon formation of the Al−O bond, while the O−O bond lengthens, resulting in energy release into many degrees of freedom. On the other hand, the recoiling O atom has initially the character of an O^- ion, but loses that extra electron on the outgoing trajectory. Therefore, a charge-transfer process must take place, which opens many channels for energy dissipation into electronic degrees of freedom of the substrate. That such a limited amount of energy is channeled into the products is not untypical for nonadiabatic processes.

From all these experimental findings a picture arises in which both abstraction and dissociation are activated by translational energy. However, at low translational energies the abstraction process dominates. At higher translational energies, the channel to ordinary dissociative chemisorption opens and this partial sticking coefficient increases faster than that for abstraction. This scenario reconciles the singles-to-pairs ratios observed by STM[7] and the increase of abstraction reported in this work. In studies of reactions on low work function metals, it has been theoretically predicted[26] and experimentally shown[27] that abstractive chemisorption is favored for collisions with the incident molecule oriented end-on. In the case of O_2 the end-on geometry is also favorable for charge transfer.[28] Recently, Yourdshanhyan et al.[11] have calculated the ground-state O_2/Al(111) potential energy surface, finding that charge transfer to form O_2^- occurs prior to lengthening of the internal O_2 bond at a larger distance from the surface for the end-on geometry. From these arguments it follows naturally that an abstraction channel may exist. However, the question remains of what hinders the ordinary chemisorption process such that abstraction is predominant at low translational energies.

Oxygen forms a stronger bond to aluminum than to any other metal.[25] Hence, it cannot be thermodynamic reasons which prevent ordinary dissociative chemisorption. This argument is supported by all recent potential energy surface calculations.[11,12] Hence, it is necessary to suspect something which is beyond the grasp of the methods used in these calculations, namely, density functional theory using state-of-the-art spin-polarized GGA schemes. Electronically excited states and nonadiabatic coupling to these states are beyond the scope of these calculations. O_2 has a $^3\Pi$ ground state in which the degenerate π_x^* and π_y^* orbitals are populated by one electron each according to Hund's rule. When the molecule approaches in the side-on geometry, which is favorable for dissociative chemisorption, the degeneracy is lifted. The $\pi_\perp^*$ orbital, for which the π lobe

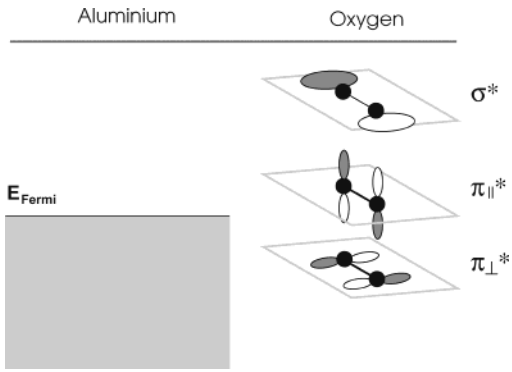

Figure 9. Molecular orbitals of O_2 in the side-on geometry interacting with a metal surface. The the $\pi_\perp$* orbital is bonding to the surface, the $\pi_{||}$* orbital is nonbonding. Initally both are filled with one electron. Upon approaching the surface, the degeneracy is lifted and for bonding both electrons should fill the $\pi_\perp$* orbital.

points toward the surface, is lower in energy and bonding toward the surface (Figure 9). The $\pi_{||}$* orbital is higher in energy and nonbonding. Hence, it is energetically favorable to transfer one electron from the $\pi_{||}$* to the $\pi_\perp$* orbital. However, this is in fact a triplet to singlet transition which is forbidden for the isolated molecule. In its interaction with the metal surface this spin transition is mediated by the spin−orbit interaction. The strength of the spin−orbit interaction scales with Z^4 of the partner, where Z is the atomic number. Hence, it may be the relatively light mass of the Al atoms which prevents this transition from occurring with the same probability as it does in the interaction with typical transition-metal surfaces. If this suggestion holds, the O_2 molecule would stay on the triplet potential energy surface, which is likely to be repulsive, when approaching the surface. At some higher energy this state may cross another state of the right symmetry and spin manifold which allows dissociative chemisorption. Thus, a sizable energy barrier would result which could corroborate the 0.2 eV barrier observed experimentally.

That the spin transitions necessary in chemisorption processes are slower than believed and can give rise to large nonadiabatic effects has been realized recently.[29] These effects are beyond the scope of present implementations of density functional theory even in its spin-polarized form, since the potentials calculated that way always collapse on the electronic ground state of given total spin, allowing the spin of the substrate to compensate for the change in spin state in the molecular subsystem, which may not be realistic. Preliminary work by Scheffler and co-workers suggests that this problem can be overcome by constraining the spin on the molecule and that under these constraints indeed a repulsive potential energy surface results.[30]

The abstraction channel is operative for the end-on geometry in which both π orbitals remain degenerate in contact with the metal surface. Moreover, this geometry allows for the most effective charge transfer to the O_2 molecule. In the interaction with O_2 this may open an alternative route to dissociation of the molecule. It should be noted that the abstraction channel is closed on most transition-metal surfaces for thermodynamic reasons. From the experimental data it is evident that rotation of the molecule during the scattering event hampers the abstraction pathway. It may be speculated that this is the case because the molecule rotates out of the favorable geometry, or alternativley because of angular momentum coupling between different electronic states.

Conclusion

Experimental data demonstrating the operation of an abstraction channel in the chemisorption of O_2 on Al(111) have been presented. The abstraction probability per scattering event is enhanced by translational energy of the incoming molecule and reduced by rotational energy of the same. The coverage dependence shows an initial induction period followed by a slow decrease of the abstraction probability. The gas-phase oxygen atoms have a translational energy about 1/7 of the excess energy from the reaction. The dependence on the angle of incidence is consistent with normal energy scaling over the limited range of angles which could be probed experimentally. Viewed together with recent STM data, our findings support that the abstraction channels dominate the dissociative events on the Al(111) surface at low translational energies. However, with increasing translational energy the yield in the ordinary chemisorption channel increases faster such that at 0.5 eV an about equal yield results. These results are interpreted to suggest that in the O_2/Al(111) interaction ordinary chemisorption is hampered because of the slow spin transition whereas the abstraction channel is open due to the large oxygen atom binding energy to Al(111), in contract to transition-metal surfaces.

Acknowledgment. We have gratefully profited from stimulating discussions with David Bird, George Darling, Stephen Holloway, Bengt Kasemo, Bruce Kay, Kurt Kolasinski, Andrew Kummel, Bengt Lundqvist, Alan Luntz, Igor Zoric, and Gerhard Ertl. We are indebt to Jörg Behler, Karsten Reuter, and Matthias Scheffler for making their results accessible to us prior to publication. We thank Olaf Weisse for his help during the final stages of the experiment. M.B. thanks the CEC for support through the TMR-program (Grant ERB FMRX-CT98-0249). Support by the Deutsche Forschungsgemeinschaft through the Schwerpunktprogramm 1093 "Dynamik von Elektronentransferprozessen an Grenzflächen" is gratefully acknowledged (Grant HA 1424/3).

References and Notes

(1) Flodström, S. A.; Martinsson, C. W. B.; Bachrach, R. Z.; Hagström, S. B. M.; Bauer, R. S. *Phys. Rev. Lett.* **1978**, *40*, 907.

(2) Zhukov, V.; Popova, I.; Yates, J. T., Jr. *Surf. Sci.* **1999**, *441*, 251.

(3) Chakarova, R.; Oner, D. E.; Zoric, I.; Kasemo, B. *Surf. Sci.* **2001**, *472*, 63. Oner, D. E.; Chakarova, R.; Zoric, I.; Kasemo, B. *J. Chem. Phys.* **2000**, *113*, 8869. Oner, D. E.; Ternow, H.; Chakarova, R.; Kasemo, B.; Zoric, I. *Surf. Sci.* **2002**, *512*, L325.

(4) Österlund, L.; Zoric, I.; Kasemo, B. *Phys. Rev. B* **1997**, *55*, 15 452.

(5) Weisse, O.; Wesenberg, C.; Binetti, M.; Hasselbrink, E.; Corriol, C.; Darling, G. R.; Holloway, S. *J. Chem. Phys.* **2003**, *118*, 8010.

(6) Hofmann, P.; Horn, K.; Bradshaw, A. M.; Jacobi, K. *Surf. Sci. Lett.* **1979**, *82*, L610.

(7) Komrowski, A. J.; Sexton, J. Z.; Kummel, A. C.; Binetti, M.; Weisse, O.; Hasselbrink, E. *Phys. Rev. Lett.* **2001**, *87*, 246103.

(8) Brune, H.; Wintterlin, J.; Behm, R. J.; Ertl, G. *Phys. Rev. Lett.* **1992**, *68*, 624. Brune, H.; Wintterlin, J.; Trost, J.; Ertl, G.; Wiechers, J.; Behm, R. J. *J. Chem. Phys.* **1993**, *99*, 2128.

(9) Schmidt, M.; Leonardelli, G.; Tscheliessnig, R.; Biedermann, A.; Varga, P. *Surf. Sci.* **2001**, *478*, L355.

(10) Dalidchik, F. I.; Grishin, M. V.; Kovalevski, S. A.; Shub, B. R. *Phys. Low-Dimens. Struct.* **2003**, *3/4*, 87.

(11) Yourdshahyan, Y.; Razaznejad, B.; Lundqvist, B. I. *Solid State Commun.* **2001**, *117*, 531.

(12) Honkala, K.; Laasonen, K. *Phys. Rev. Lett.* **2000**, *84*, 705. Sasaki, T.; Ohno, T. *Phys. Rev. B* **1999**, *60*, 7824.

(13) Eichler, A.; Hafner, J. *Phys. Rev. Lett.* **1998**, *79*, 4481. Mittendorfer, F.; Eichler, A.; Hafner, J. *Surf. Sci.* **1999**, *435*, 756.

(14) Hellman, A.; Razaznejad, B.; Yourdshahyan, Y.; Ternow, H.; Zoric, I.; Lundqvist, B. I. *Surf. Sci.* **2003**, *532*, 126.

(15) Engdahl, C.; Wahnström, G. *Surf. Sci.* **1994**, *312*, 429.
(16) Wahnström, G.; Lee, A. B.; Strömquist, J. *J. Chem. Phys.* **1996**, *105*, 326.
(17) Binetti, M.; Weisse, O.; Hasselbrink, E.; Komrowski, A. J.; Kummel, A. C. *Faraday Discuss. Chem. Soc.* **2000**, *117*, 313.
(18) Binetti, M.; Weisse, O.; Hasselbrink, E.; Katz, G.; Kosloff, R.; Zeiri, Y. *Chem. Phys. Lett.* **2003**, *373*, 366.
(19) Hasselbrink, E.; Jakubith, S.; Nettesheim, S.; Wolf, M.; Cassuto, A.; Ertl, G. *J. Chem. Phys.* **1990**, *92*, 3154.
(20) Goldsmith, J. E. M. *J. Chem. Phys.* **1983**, *78*, 1610. Bamford, D. J.; Jusinski, L. E.; Bischel, W. K. *Phys. Rev. A* **1986**, *34*, 185. Bamford, D. J.; Dyer, M. J.; Bischel, W. K. *Phys. Rev. A* **1987**, *36*, 3497.
(21) Bujisse, B.; Zande, W. J. v. d.; Eppink, A. T. J. B.; Parker, D. H.; Lewis, B. R.; Gibson, S. T. *J. Chem. Phys.* **1998**, *108*, 729.
(22) Mettes, J.; Heijmen, B.; Reuss, J.; Laine, D. C. *Chem. Phys.* **1984**, *87*, 1.
(23) Andresen, P.; Faubel, M.; Häusler, D.; Kraft, G.; Lülf, H.-W.; Skofronick, J. G. *Rev. Sci. Instrum.* **1985**, *56*, 2038. Joswig, H.; Andresen, P.; Schinke, R. *J. Chem. Phys.* **1986**, *85*, 1904.
(24) Michelsen, H. A.; Rettner, C. T.; Auerbach, D. J. *Phys. Rev. Lett.* **1992**, *69*, 2678. Michelsen, H. A.; Rettner, C. T.; Auerbach, D. J.; Zare, R. N. *J. Chem. Phys.* **1993**, *98*, 8294. Beutl, M.; Riedler, M.; Rendulic, K. D. *Chem. Phys. Lett.* **1995**, *247*, 249.
(25) Jacobsen, J.; Hammer, B.; Jacobsen, K. W.; Nørskov, J. K. *Phys. Rev. B* **1995**, *55*, 14 954.
(26) Strömquist, J.; Hellberg, L.; Kasemo, B.; Lundqvist, B. I. *Surf. Sci.* **1996**, *352/4*, 435.
(27) Brandt, M.; Kuhlmann, F.; Greber, T.; Böwering, N.; Heinzmann, U. *Surf. Sci.* **1999**, *439*, 49.
(28) Teillet-Billy, D.; Bahrim, B.; Gauyacq, J. P. *Nucl. Instrum. Methods Phys. Res., B* **1995**, *100*, 296.
(29) Trail, J. R.; Graham, M. C.; Bird, D. M.; Persson, M.; Holloway, S. *Phys. Rev. Lett.* **2002**, *88*, 166802. Trail, J. R.; Bird, D. M.; Persson, M.; Holloway, S. *J. Chem. Phys.* **2003**, *119*, 4539.
(30) Behler, J.; Lorenz, S.; Delley, B.; Reuter, K.; Scheffler, M. To be published.